

Collisional radiative model for heavy atoms in hot non-local-thermodynamical-equilibrium plasmas

A. Bar-Shalom,* J. Oreg,* and M. Klapisch[†]
ARTEP Inc., Columbia, Maryland 21045

(Received 18 April 1997)

A collisional radiative model for calculating non-local-thermodynamical-equilibrium (non-LTE) spectra of heavy atoms in hot plasmas has been developed, taking into account the numerous excited and autoionizing states. This model uses superconfigurations as effective levels with an iterative procedure which converges to the detailed configuration spectrum. The non-LTE opacities and emissivities may serve as a reliable benchmark for simpler on-line models in hydrodynamic code simulations. The model is tested against detailed configuration calculations of selenium and is applied to non-LTE optically thin plasma of lutetium. [S1063-651X(97)51307-9]

PACS number(s): 52.25.Nr, 31.15.Bs, 52.25.Vy

Radiation hydrodynamical simulations of laser produced plasmas require knowledge of the level populations of ions through their average charge Z^* , their ionization energy, and their radiative properties. This knowledge is also necessary to interpret the emission spectra from hot laboratory and astrophysical plasmas. A common approximation in these problems has been to assume local thermodynamical equilibrium (LTE), i.e., Saha-Boltzmann populations. The LTE approximation was used, for example, to develop the super transition array (STA) theory [1,2]. However, non-LTE effects are of dramatic importance to laser produced plasmas [3,4], because of the strong laser energy deposition at the surface of the target. To go beyond LTE, one needs a collisional radiative model (CRM) [5], which requires transition rates between all levels.

For medium and heavy ions of interest in laser fusion and x-ray lasers there are multiple charge states and numerous excited and autoionizing manifolds. Although some highly efficient computational methods have been developed in the last decade [6], there still needs to be some type of averaging procedure to treat the numerous excited configurations. In this paper we present a model that is based upon the same method as the STA theory, using superconfigurations (SCs) [1,2] as effective levels with a rapidly convergent procedure that provides the detailed configuration non-LTE spectrum in the limit. This model, called superconfiguration radiative collisional (SCROLL), calculates the effect of the numerous excited and autoionizing states on ionization balance and spectra of heavy elements. Furthermore, SCROLL provides accurate and detailed non-LTE opacities and emissivities that can serve as reliable benchmarks in the development of simpler and faster on-line models that can be used in numerical simulations of radiation hydrodynamics.

A superconfiguration (SC) groups together numerous configurations of similar energies [1,2]. It is constructed from supershells σ , which are unions of energetically adjacent ordinary atomic subshells $s \in \sigma$, $s \equiv \mathbf{j}_s \equiv n_s l_s j_s$. A SC is de-

finied by a set of supershell occupation numbers Q_σ . In a Q -electron ion we have $\sum_\sigma Q_\sigma = Q$. The Q_σ electrons are distributed among the subshells $s \in \sigma$ in all possible ways subject to $\sum_{s \in \sigma} q_s = Q_\sigma$. Thus, each partition $\mathcal{P} = \mathcal{P}(Q)$ is a set of q_s generating an ordinary configuration $C = \prod_s \mathbf{j}_s^{q_s}$.

For a given supershell structure (i.e., a particular grouping of ordinary shells into supershells), the collection of all possible occupations Q_σ for all supershells σ , restricted by $\sum_\sigma Q_\sigma = Q$, includes all the superconfigurations of charge state $Z-Q$. With the less restrictive condition $\sum_\sigma Q_\sigma \leq Z$, this collection includes all the SCs of all ions of element Z . The model rate equations are

$$\frac{dN_{\Xi}}{dt} = -N_{\Xi} \sum_{\Xi'} R_{\Xi\Xi'} + \sum_{\Xi'} N_{\Xi'} R_{\Xi'\Xi}, \quad (1)$$

where N_{Ξ} are the SC populations and $R_{\Xi\Xi'}$ are the SC transition rates, averaged over the initial configurations $C \in \Xi$ and summed over all final $C' \in \Xi'$. A central assumption in our model is that within a superconfiguration Ξ , the configuration populations N_C are distributed according to the Saha-Boltzmann statistics: $N_C/N_{\Xi} = U_C/U_{\Xi}$, where U_C and $U_{\Xi}(g) \equiv \prod_\sigma U_\sigma(g)$ are the corresponding partition functions [1], and where (g) stands for the set of degeneracies $\{g_s\}$ of the various shells. Here,

$$U_\sigma(g) \equiv \sum_{\mathcal{P}} \prod_{s \in \sigma} \binom{g_s}{q_s} X_s^{q_s}, \quad (2)$$

with $X_s \equiv e^{-(\varepsilon_s - \mu)/kT}$, where ε_s is the shell energy and μ is the chemical potential. The Saha-Boltzmann assumption, which is strictly valid under LTE conditions only, is relaxed effectively by a convergence procedure, performed by splitting supershells as described below. The SC average rates can thus be written as

*Permanent address: NRCN, P.O. Box 9001, Beer-Sheva, Israel.

[†]Mailing address: NRL code 6730, Washington, DC 20375.

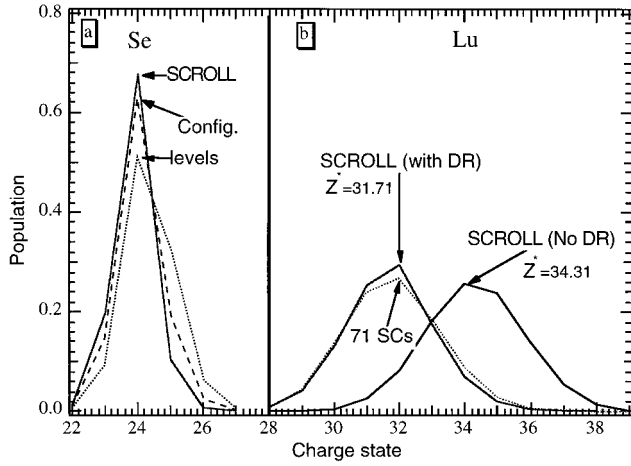


FIG. 1. (a) The charge distribution of Se at $T_e=700$ eV, $N_e=5 \times 10^{20}$ cm $^{-3}$. Comparison of the SCROLL results with detailed calculation [10]. (b) The effects of convergence and autoionization on the charge distribution of Lu at $T_e=400$ eV, $N_e=5 \times 10^{20}$ cm $^{-3}$.

$$R_{\Xi\Xi'} \equiv \frac{1}{U_{\Xi}(g)} \sum_{\substack{C \in \Xi \\ C' \in \Xi'}} U_C R_{CC'}, \quad (3)$$

where $R_{CC'}$ are the configuration average rates. We first express the latter as $R_{CC'} = P_{CC'}(q)B(\mathbf{j})$ where $P_{CC'}(q)$ is the occupation number polynomial

$$P_{CC'}(q) = q_{\alpha}^{n_{\alpha}} (g_{\beta} - q_{\beta})^{n_{\beta}} (q_{\gamma} - \delta_{\alpha\gamma})^{n_{\gamma}} \quad (4)$$

and α , β , and γ are the active orbitals. The exponents for the various processes are $n_{\alpha} = n_{\beta} = 1$ and $n_{\gamma} = 0$ except for ionization where $n_{\beta} = 0$, and except for autoionization for which $n_{\gamma} = 1$. The remainder part $B(\mathbf{j})$ is the ‘‘orbital rate’’ specific for each process and depends only on the orbital wave functions. After factorization of the continuum [6], the only two-electron contribution is autoionization involving a continuum orbital $\tilde{\mathbf{j}}$ for which we obtained

$$B(\mathbf{j}) = \frac{1}{g_{\alpha} g_{\beta} (g_{\gamma} - \delta_{\alpha\gamma})} \sum_{tt'} \left[\frac{\delta_{tt'}}{2t+1} + \begin{Bmatrix} j_{\alpha} & j_{\beta} & t \\ j_{\gamma} & \tilde{\mathbf{j}} & t' \end{Bmatrix} \Phi^{tt'}(\mathbf{j}_{\alpha} \mathbf{j}_{\beta} \mathbf{j}_{\gamma} \tilde{\mathbf{j}}) \right], \quad (5)$$

where $\Phi^{tt'}$ is a product of radial integrals including both direct and exchange contributions [6].

For any process and transition, the $B(\mathbf{j})$'s are common to all configurations within a SC array and we have $R_{\Xi\Xi'} = B(\mathbf{j})P_{\Xi\Xi'}$. Using partition function algebra [1] one obtains

$$P_{\Xi\Xi'} = \frac{U_{\Xi}(g)}{U_{\Xi'}(g)}, \quad (6)$$

where $U_{\Xi}(g) = U_{\Xi}(g^{(n_{\alpha} n_{\beta} n_{\gamma})})$ is a generalized partition function (GPF) defined formally in the same way as $U_{\Xi}(g)$ of Eq. (2) but with the modified shell degeneracies

$$(g^{(n_{\alpha} n_{\beta} n_{\gamma})})_s \equiv g_s - \sum_{\eta=\alpha,\beta,\gamma} n_{\eta} \delta_{s\eta} \quad (7)$$

and with $\Xi^{(n_{\alpha} n_{\beta} n_{\gamma})}$ having the supershell occupation numbers Q_{σ} reduced by n_{α} and/or n_{β} for σ containing α and/or β , respectively. The calculation of GPFs bypasses the impractical direct summations by a set of recursion formulas [1]. The ‘‘orbital rates’’ $B(\mathbf{j})$ are calculated with the MICCRON code [7].

The assumption of LTE within SCs is relaxed by a convergence procedure where in each step *supershells* are split, giving rise to a new set of SCs of all charge states in Eq. (1) as described below. After each splitting the initial population of the new SCs is taken as proportional to their partition functions. All the rates between the new SCs of all charge states are computed and the steady-state CRM matrix is rebuilt and solved with a sparse matrix method. The resulting populations are then compared to the initial ones. The supershells are split in this way repeatedly, until all N_{Ξ} converge.

It should be pointed out that in order to achieve rapid and systematic convergence we do not split SCs but rather supershells. When a supershell σ_0 is split into two supershells $\sigma_0 \rightarrow \sigma_1 \sigma_2$, e.g., $(2s2p3s3p3d) \rightarrow (2s2p)(3s3p3d)$, each SC possessing Q_{σ_0} electrons on supershell σ_0 gives now rise to many ‘‘smaller’’ SCs defined by *all* Q_{σ_1} and Q_{σ_2} for which $Q_{\sigma_1} + Q_{\sigma_2} = Q_{\sigma_0}$ (together with the Q_{σ} of the other supershells). Therefore a gradual supershell splitting yields jumps in the number of SCs generated. Supershells are split sequentially according to their energy width and occupation number.

This convergence process eliminates gradually the explicit dependence of the rates (3) on the LTE Boltzmann factors in U_C . In the configuration limit it disappears completely. Ignoring the first order energy corrections in the Boltzmann factors of Eq. (3) has therefore little effect on the converged results. During these iterations a great simplifica-

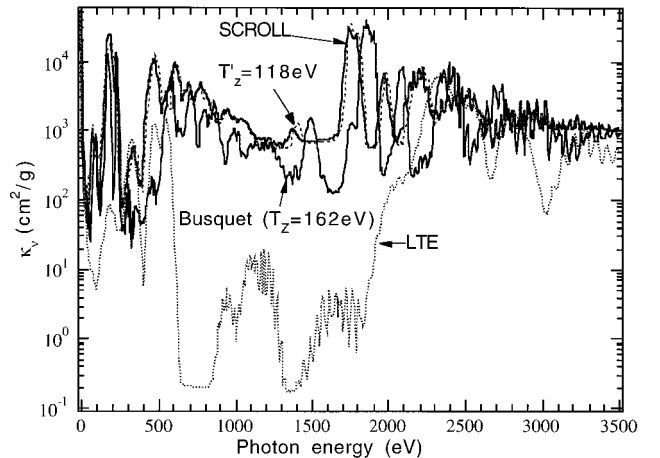


FIG. 2. Absorption spectra of Lu plasma at $T_e=400$ eV, $N_e=10^{20}$ cm $^{-3}$. Comparison between SCROLL and various LTE models.

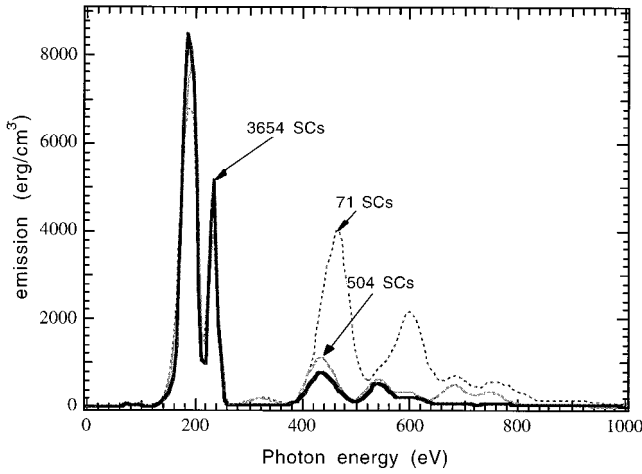


FIG. 3. Emission spectrum of Lu plasma at $T_e=400$ eV, $N_e=10^{20}$ cm^{-3} showing sensitivity to the degree of convergence of SC populations in SCROLL.

tion is achieved by using an average atom potential depending on Z^* which is kept constant. An outer convergence loop on Z^* is then performed. Rapid convergence for both N_{Ξ} and the average charge Z^* is achieved easily, thanks to the high multiplicity of excited configurations which turns out here to be an advantage. In our calculations we keep track of all charge states whose population exceeds 10^{-5} of the total ion population. We accounted for all the SCs (of all these charge states) involving principal quantum numbers up to $n=8$, or less according to pressure ionization. In general (e.g., see Fig. 1) about ten ionization stages contribute to the charge distribution and spectra. It was found [8] that the charge distribution can be described by an ionization temperature T_z defined as $Z_{\text{LTE}}^*(T_z) = Z_{\text{non-LTE}}^*(T_e)$.

It is important to emphasize here that the supershell structure, which suffices for the SC population convergence, is not sufficient for revealing the spectral details. Indeed to obtain the detailed absorption spectrum κ_ν , we now take the SCROLL converged set of SCs, Ξ^{scroll} , and their populations as the initial set for a modified STA code [1,2] at the converged T_z value. Supershells are further split assuming LTE populations within Ξ^{scroll} , giving rise to increasing number of smaller transition arrays $\Xi \Rightarrow \Xi'$ (STAs) each represented by a Gaussian. The splitting of supershells continues until the spectrum is converged. The limit, where each supershell is a single ordinary shell, gives the detailed configuration spectrum. The non-LTE features enter through scaling each STA Gaussian by the non-LTE population $N_{\Xi^{\text{scroll}}}^{\text{non-LTE}}$ of its initial parent Ξ^{scroll} , as obtained from the SCROLL rate equation (1). The absorption spectrum κ_ν is then obtained by superposing all these scaled STAs convolved with the Voigt profile of an individual line. The bound-free contribution [2] includes integration over the Maxwellian distribution of the free electrons. *It is important to note here that the first three moment of the STA Gaussians, total intensity, average energy, and variance, are calculated [1] using optimized potentials (orbital relaxation) and including first-order correction to the Boltzmann factors, configuration widths, and configuration interaction.*

It is well known [9] that the source function connecting the emissivity j_ν with the net opacity reduces to the Planck

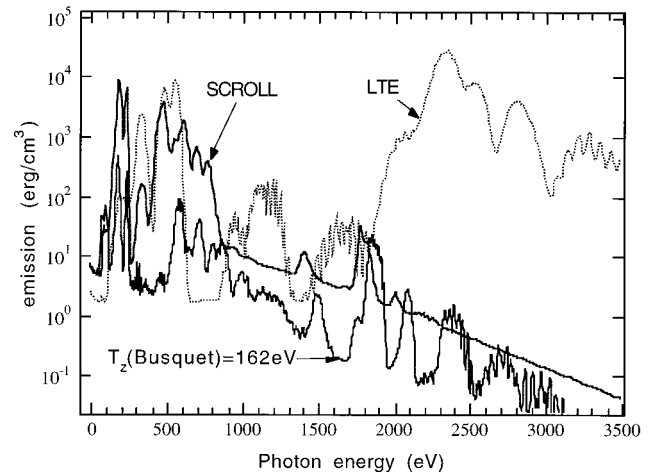


FIG. 4. Emissivity of Lu plasma at $T_e=400$ eV, $N_e=10^{20}$ cm^{-3} . Comparison between SCROLL and LTE results at $T_e=400$ eV and at $T_z=162$ eV.

function under LTE conditions. In the SCROLL model the source function requires special attention. Taking into account the non-LTE populations $N_{\Xi^{\text{scroll}}}^{\text{scroll}}$, the LTE behavior with effective T_z within Ξ^{scroll} , and the fact that free electrons have a Maxwellian distribution at the real temperature T_e , we obtain a source function $S(\nu) = j_\nu / \kappa_\nu$ for each array $\Xi^{\text{scroll}} \rightarrow \Xi', \text{scroll}$ as

$$S_{\Xi^{\text{scroll}} \rightarrow \Xi', \text{scroll}}(\nu) = \frac{2h\nu^3}{c^2} f_{\Xi^{\text{scroll}} \rightarrow \Xi', \text{scroll}}^{bb} e^{-h\nu/kT_z} \quad (8)$$

where for the bound-bound spectrum $f_{\Xi^{\text{scroll}} \rightarrow \Xi', \text{scroll}}^{bb} \equiv N_{\Xi^{\text{scroll}}}^{\text{scroll}} N_{\Xi'}^{\text{LTE}} / N_{\Xi'}^{\text{LTE}} N_{\Xi^{\text{scroll}}}^{\text{scroll}}$ and for the bound free spectrum $f_{\Xi^{\text{scroll}} \rightarrow \Xi', \text{scroll}}^{bf} \equiv f_{\Xi^{\text{scroll}} \rightarrow \Xi', \text{scroll}}^{bb} (T_z/T_e)^{3/2} e^{-\varepsilon/kT^*}$. Here the LTE populations are taken at $T=T_z$ and $T^{*-1} \equiv T_e^{-1} - T_z^{-1}$, and ε is the free-electron energy. This term enters the above-mentioned integration over ε [2]. The free-free spectrum involves only the LTE free-electron distribution and its source function is the Planck function at T_e .

Results for both absorption and emission are presented below. In Fig. 1(a) we compare the converged SCROLL results for the charge distribution with detailed configurations and detailed levels calculations [10] for the selenium case, at $T_e=700$ eV and $N_e=5 \times 10^{20}$ cm^{-3} , where such detailed calculations are possible. It is seen that the SCROLL result agrees with the detailed configuration result. The effect of averaging over configurations is shown by comparison with the detailed level result. The higher ionization of the detailed levels results is due to the metastable states of Ne-like $2p^5 3s$, which are easily ionized; this cannot be reproduced in an averaged picture. The convergence is shown in Fig. 1(b) for Lu at $T_e=400$ eV, $N_e=10^{20}$ cm^{-3} . The result of 71 SCs (for all charge states) nearly reproduce that of 3654 SCs with the respective Z^* 31.81 and 31.71. Similar convergence is obtained for the absorption spectrum with the respective Rosseland means (κ_R) 1077 and 1088 cm^2/g .

The non-LTE absorption spectrum of this Lu plasma is shown in Fig. 2. The strong non-LTE effect, of orders of magnitude, is striking here. The LTE κ_R is only 1.2 cm^2/g and the average charge is $Z^*=53.69$. Busquet's

model [8,4], which predicts an effective ionization temperature of $T_z=162$ eV, improves the agreement with a $\kappa_R=460$ cm²/g, and $Z^*=38.49$. However, it is seen that the SCROLL absorption spectrum can be reproduced more accurately by a different effective ionization temperature of $T'_z=118$ eV, which gives $\kappa_R=1025$ cm²/g, $Z^*=32.09$, in remarkable agreement with SCROLL. This result is due to the insensitivity of the low levels populations, from which absorption originates, to the various models. These last results may be of crucial significance since effective temperature LTE models are easily applied in on-line hydrodynamic simulations.

On the other hand, the emissivity shows greater sensitivity to the detailed structure of the excited SCs, which have relatively small populations. This appears clearly in Fig. 3, showing the emission spectrum of Lu in the same conditions, for various convergence stages with 71, 504, and 3654 SCs (all charge states). The same effect is seen in Fig. 4 comparing SCROLL with the simpler models mentioned above. For emission unlike absorption, the $T_z=118$ eV spectrum (omitted here for clarity) does not reproduce the SCROLL converged results (3654 SCs). This shows that an accurate and elaborate model such as SCROLL is necessary for the computation of radiation of hot plasmas. The SCROLL results may provide a guide to possible improvements to Busquet's model. A detailed discussion of this important model in comparison with SCROLL is given in Ref. [4]. Finally, the

SCROLL model provides a quantitative estimate of the contribution of the autoionizing levels whose detailed accounting is impractical for heavy elements. The charge distribution plotted in Fig. 1(b) shows a significant shift due to dielectronic recombination (DR) and the average charge Z^* changes from 31.71 to 34.31 when DR is excluded.

In summary we have presented a non-LTE collisional radiative model that takes into account the numerous excited levels of heavy ions in hot plasmas. The model gives the detailed opacity, emissivity, and charge distribution, and is applicable to any atom. We have presented results for steady-state thin plasmas of Se and Lu, demonstrating the success of the model in providing rapid convergence to the detailed configuration results. The SCROLL model may serve to check and improve the applicability of the much simpler model of Busquet which is used in on-line hydrodynamic simulations. The extension of the SCROLL model to include detailed (possibly metastable) levels is in progress.

We thank Dr. Al Osterheld for allowing us to use his detailed calculations of the Se system. We also thank Dr. S. E. Bodner for his comments and encouragement. This research was performed while the authors resided at the Naval Research Laboratory in Washington, D.C. The research was funded by NRL, from its contract with the Department of Energy.

-
- [1] A. Bar-Shalom, J. Oreg, W. H. Goldstein, D. Shvarts, and A. Zigler, *Phys. Rev. A* **40**, 3183 (1989); A. Bar-Shalom, J. Oreg, and W. H. Goldstein, in *Radiative Properties of Hot Dense Matter*, edited by W. H. Goldstein, C. Hooper, J. Gautier, J. Seely, and R. Lee (World Scientific, Singapore, 1991), p. 163; A. Bar-Shalom, J. Oreg, and W. H. Goldstein, in *Atomic Processes in Plasmas*, edited by E. S. Marmor and J. L. Terry (AIP, New York, 1991), p. 68; *J. Quant. Spectrosc. Radiat. Transf.* **51**, 27 (1994); *Phys. Rev. E* **51** 4882 (1995); J. Oreg, A. Bar-Shalom, and M. Klapisch, *Phys. Rev. E* **55**, 5874 (1997).
- [2] A. Bar-Shalom and J. Oreg, *Phys. Rev. E* **54**, 1850 (1996).
- [3] R. L. Kauffman, LLNL, Laser Prog. annual report No. UCRL 50021-85, 1985 (unpublished).
- [4] M. Klapisch and A. Bar-Shalom, *J. Quant. Spectrosc. Radiat. Transf.* (to be published).
- [5] D. R. Bates, A. E. Kingston, and R. W. P. McWhirter, *Proc. R. Soc. London, Ser. A* **267**, 297 (1962); R. W. P. McWhirter, *Phys. Rep.* **37**, 165 (1978).
- [6] A. Bar-Shalom, M. Klapisch, and J. Oreg, *Phys. Rev. A* **38**, 1773 (1988); *Comput. Phys. Commun.* **93**, 21 (1996).
- [7] MICRON is an extension of the HULLAC code to cases of several charge states; see Ref. [4].
- [8] M. Busquet, *Phys. Fluids B* **5**, 4191 (1993).
- [9] D. Mihalas, *Stellar Atmospheres* (Freeman and Co., San Francisco, 1978).
- [10] A. Osterheld, R. S. Walling, B. K. F. Young, W. H. Goldstein, G. Shimkaveg, B. J. MacGowan, L. DaSilva, R. London, D. Matthews, and R. E. Stewart, *J. Quant. Spectrosc. Radiat. Transf.* **51**, 263 (1994).